JOURNAL OF Applied Polymer SCIENCE

Novel Kind of Functional Gradient Poly(ε-caprolactone) Polyurethane Nanocomposite: A Shape-Memory Effect Induced in Three Ways

Yan Cai, Xin Feng, Ji-Sen Jiang
Department of Physics, Center of Functional Nanomaterials and Devices, East China Normal University, Shanghai 200241, China
Correspondence to: J.-S. Jiang (E-mail: jsjiang@phy.ecnu.edu.cn)

ABSTRACT: Multiwalled carbon nanotube (MWCNT) crosslinked polyurethane nanocomposites filled with iron (Fe) powders were synthesized by an *in situ* polymerization method. The Fe powders were deposited on one side of the nanocomposites during sample formation. Because of the gradient distribution of the Fe powders, the polymer part was affected little; this resulted in good mechanical properties of the nanocomposites. The electrical conductivities on each side of the nanocomposites were different. Because of the good magnetic properties and high electrical conductivities of the nanocomposites, the shape-memory effect could be induced by temperature heating (temperature = 45°C), electrically resistive Joule heating (voltage (U) = 30 V), and magnetic field heating (frequency (f) = 45 kHz, intensity of magnetic field (H) = 46.5 kA/m). The shape-memory properties were dependent on the location of the side that contained the most Fe powders (Fe side), and the nanocomposites showed better shape-memory properties when the Fe side was located inside of the folded samples. © 2013 Wiley Periodicals, Inc. J. Appl. Polym. Sci. **2014**, *131*, 40220.

KEYWORDS: magnetism and magnetic properties; mechanical properties; polyurethanes; synthesis and processing

Received 12 September 2013; accepted 22 November 2013
DOI: 10.1002/app.40220

INTRODUCTION

During the past few years, shape-memory polymers (SMPs), which can sense and respond to an external stimulus, have drawn more and more attention for their novel properties. They have many advantages in terms of their light weight, low cost, easy processing, and so on.[1] Generally, pure SMPs are thermo-induced materials for which the shape-memory effect (SME) can be induced by a hot liquid or gas.[2,3] Nowadays, many researches are aiming to develop new SMP composites that are filled with functional fillers and natural materials.[4–7] Thus, the SME can be induced by several external stimuli, including temperature heating,[8,9] infrared light heating,[10] Joule heating,[11–13] and magnetic field heating.[14–17] Voltage triggering and magnetic field triggering are two convenient inductive heating methods. The SME of the SMP composites may be realized by heating from inside the particles under specific conditions.

Because of the power loss of magnetic particles, such as iron (II,III) oxide (Fe_3O_4)[18,19] and nickel zinc ferrite ferromagnetic particles[20] in alternating magnetic fields, a noncontact triggering of SEM can be realized. Golbang and Kokabi[16] synthesized a kind of nanoclay/NdFeB/crosslinked low-density polyethylene shape-memory nanocomposite. Good shape-memory properties were explored in an alternative magnetic field with a frequency of 9 kHz and a strength of 15 kW. Kumar et al.[21] incorporated silica-coated iron oxide particles into a polymer network matrix, which was made of poly(ε-caprolactone) (PCL) and poly(cyclohexyl methacrylate) segments, and the SME in an alternating magnetic field (f = 258 kHz) was successfully realized. However, at a high content of magnetic particles, such as Fe_3O_4, SMP nanocomposites will be brittle.[18,19,22] Thus, the application of SMP composites may be restricted. The question of how to improve the mechanical properties of SMP composites is still a big challenge. Lu et al.[23] incorporated carbon nanofiber (CNF) nanopaper on the surface of SMP composites during the formation process and found that the fillers had little influence on the polymer matrix. Therefore, if magnetic particles can be located on the surface of the composites as well, the SMP nanocomposites may have good mechanical properties at a high content of magnetic particles.

Traditional polymers (plastic) are electrical insulators that have a low conductivity. Fortunately, the introduction of highly conductive materials into the polymer matrix is an effective way to improve the conductivity. For example, electroactive SMPs are prepared by the incorporation of inducting fillers such as carbon black (CB),[24,25] carbon nanotubes (CNTs),[13,26] CNFs,[12,23,27] and other electrically conducting materials. Because carbon materials are highly conductive, once they are introduced into the polymer matrix, the electrical resistance will be significantly reduced. Thus, the SME can be triggered by means of Joule heating. Yu et al.[24] synthesized a kind of CNT/CB/shape-

memory nanocomposite. Through the application of an electric field during sample formation, CNTs (1.0 wt %) were electrically induced into aligned chains in polymer composites. They served as long-distance conductive channels to bridge the CB aggregations. The electrical resistivities of the samples significantly decreased by more than 100 times. The composite blended with 15 wt % CB and 1 wt % chained CNTs had an electroactive shape-recovery behavior in response to 25 V electrical voltages. Lee and Yu[11] prepared a kind of single-walled CNT/polyurethane nanocomposite. They found that when 30 V electrical voltages were applied, the shape-recovery time of the sample was 90 s, and the shape-recovery rate (R_r) was 88%. In addition to carbon materials, metals such as copper (Cu), nickel (Ni), and iron (Fe) are good conductive materials. A kind of shape-memory nanocomposite filled with CNFs and submicrofilamentary nickel nanostrands was prepared by Lu et al.[28] The combination of CNFs and Ni nanostrands significantly improved the electrical conductivities. Under a constant direct-current (dc) voltage of 36 V, a deformed SMP nanocomposite, which was integrated with 2.5 wt % CNFs and 7.5 wt % nanostrands, recovered its original shape in 1 min. As is known to all, Ni and Fe have good magnetic properties, which can be orderly arranged under a magnetic field. Leng et al.[29] had incorporated micrometer sized Ni powders into a thermo responsive shape-memory polyurethane. During the process of sample preparation, they used a weak static magnetic field (0.03T) to form conductive Ni chains in the polymer. Hence, the electrical conductivities of the SMP nanocomposites in the chain direction were improved significantly, and the SMP nanocomposites were suitable for electroactive shape recovery.

Nowadays, some researchers have introduced magnetic particles into electroactive SMP nanocomposites. The SME is successfully realized under a certain dc voltage. However, researchers have not explored the magnetically induced SME of the same sample yet. So in this study, we explored whether a kind of SMP nanocomposite could be induced by temperature heating, Joule heating, and magnetic field heating. As a result, a new system of multiwalled carbon nanotube (MWCNT) crosslinked polyurethane shape-memory nanocomposite filled with Fe powder was prepared. In the prepared nanocomposites, the MWCNTs were used as crosslinking agents, and the Fe powders were deposited on one side of the nanocomposites; this resulted in a gradient distribution of Fe powders in the nanocomposites. The thermal properties, mechanical properties, magnetic properties, and electrical conductivities of the Fe/MWCNT-crosslinked polyurethane functional gradient nanocomposites were studied systematically. We hoped that the nanocomposites would have good mechanical properties and their SME could be induced by three ways: temperature heating, Joule heating, and magnetic field heating.

EXPERIMENTAL

Materials

PCL diol (number-average molecular weight = 5000 g/mol) was synthesized in our laboratory.[18] MWCNTs with a diameter range of 10–20 nm, a length range of 10–30 μm, and a purity over 95% were purchased from Chengdu Organic Chemicals Co., Ltd. (Chinese Academy of Sciences) and were treated by nitric acid.[30] Reduced Fe powders were purchased from Shanghai Jinshan Smelter. 4,4′-Diphenylmethane diisocyanate (MDI; 98%, Alfa Aesar) was used directly. Dimethylformamide (DMF; analytical reagent) was dried over calcium hydroxide and was distilled before use. Other relative regents were purchased from local agent companies.

Preparation of the Functional Gradient Fe/MWCNT-Crosslinked Polyurethane Nanocomposites

The functional gradient Fe/MWCNT-crosslinked polyurethane nanocomposites were prepared by *in situ* polymerization. The molar ratio of PCL to MDI was 1:4, and the content of MWCNTs was 0.5 wt % (relative to the monomer mixture). Nanocomposites filled with different contents of Fe powders were prepared by the following steps. First, a certain amount of PCL diol, Fe powder, and MWCNTs were dispersed in a certain volume of DMF. The mixture was heated at 70°C for 30 min with mechanical stirring. Second, stannous octoate (0.1 wt % of PCL diol, g/g) in dried DMF and a given amount of MDI were added to the mixture. Subsequently, the mixture was stirred for 20 min at 70°C and for 1.5 h at 90°C. Third, the mixture was stirred at 110°C for 2.5 h. In the end, the mixture was put into a glass plate and dried at 80°C *in vacuo* for 24 h and at 60°C for 48 h. Thus, 1–2 mm thick SMP nanocomposites were obtained. SMP nanocomposites blended with various contents of Fe powders were named with their weight concentrations as PCF3 (30 wt % Fe powder), PCF4 (40 wt % Fe powder), and PCF5 (50 wt % Fe powder), respectively.

Measurements

A Fourier transform infrared (FTIR) spectrophotometer (Nexus 670, Nicolet) was used to analyze the structures of PCF3, PCF4, and PCF5. The thermal properties of the nanocomposites were studied by differential scanning calorimetry (DSC) analysis (DSC2910, TA Instruments). The testing samples weighed around 10 mg, the constant heating rate was 10°C/min from −10 to 150°C, and the samples were purged with nitrogen. The dispersion of particles in PCF5 was studied with field emission scanning electron microscopy (FESEM; S4800, Hitachi, Japan). A universal testing machine (Instron RG 3010, China) was used to test the mechanical properties of the nanocomposites at room temperature. Each dumbbell-type sample was tested three times. A magnetic measurements variable field translation balance (Petersen, Germany) was used to record the magnetization curves of the samples at room temperature. A Hall effect measurement system (HMS-3000, Korea) was used to measure the electrical conductivities of each sample.

A fold-deploy shape-memory test[22,31] was carried out to study the shape-memory properties of the nanocomposites under different conditions. Figure 1 exhibits a schematic drawing of a folded sample. Because the Fe powders showed a gradient distribution in the nanocomposites, the shape-memory properties of the nanocomposites were studied in two ways, in which the Fe side was located both inside and outside of the folded samples. The shape-memory properties of PCF3, PCF4, and PCF5 were induced by three ways: temperature heating, Joule heating, and magnetic field heating. A temperature of 45°C was chosen as a

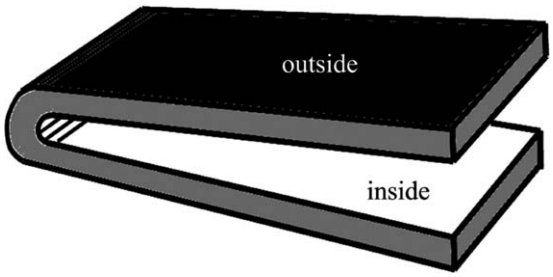

Figure 1. Schematic drawing of a folded sample.

thermotransition temperature (T_{trans}). The alternating magnetic field was provided by an inductive heating machine (SP-15A, Shenzhen, China). A constant dc voltage of 30 V was offered by a dc power supply (SW-17WYJ, Shanghai, China). The shape-recovery process was recorded by a digital camera, and each sample (30 × 10 × 1 mm^3, Length × Width × Thickness) was tested for three times. An infrared thermometer was used to measure the temperature of these samples during the shape-recovery process. The shape retention rate (R_f) and R_r were calculated with eqs. (1) and (2):

$$R_f(\%) = \frac{180^\circ - \theta_f}{180^\circ} \times 100 \quad (1)$$

$$R_r(\%) = \frac{\theta_r}{180^\circ} \times 100 \quad (2)$$

where θ_f is the angle of the folded samples after they were exposed to room temperature for 5 min and θ_r is the final angle after one shape-recovery process.

RESULTS AND DISCUSSION

The FTIR spectra of the nanocomposites PCF3, PCF4, and PCF5 are shown in Figure 2(a–c). As shown in Figure 2, the N—H stretching vibration peak appeared at 3364 cm^{-1}, and the peak at 1534 cm^{-1} was due to N—H deformation. The peak at 1731 cm^{-1} was attributed to the C=O bond. The peaks located at 2942 and 2865 cm^{-1} were the CH_2 symmetric and asymmetric stretching vibrations, respectively.[32] The FTIR results confirmed the structure of the polyurethane nanocomposites, and

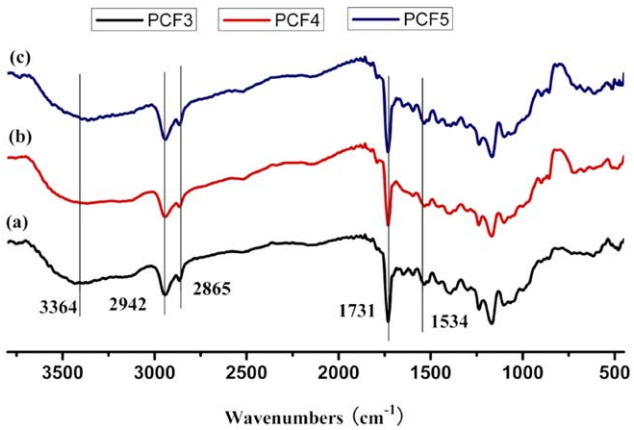

Figure 2. FTIR spectra of the samples: (a) PCF3, (b) PCF4, and (c) PCF5. [Color figure can be viewed in the online issue, which is available at wileyonlinelibrary.com.]

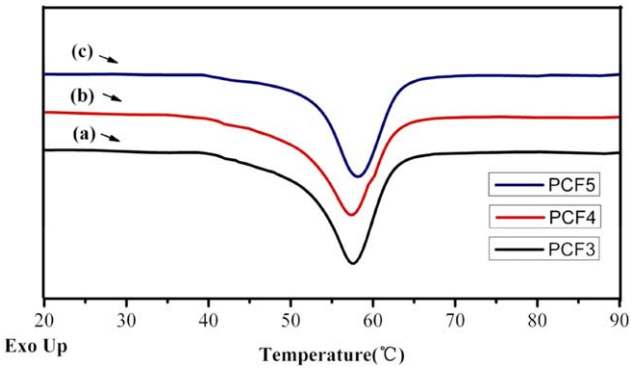

Figure 3. DSC second curves of the samples: (a) PCF3, (b) PCF4, and (c) PCF5. [Color figure can be viewed in the online issue, which is available at wileyonlinelibrary.com.]

this indicated that the preparation of the nanocomposites was successful.

The thermal properties of the nanocomposites were analyzed with the DSC results. Figure 3 shows the DSC second thermogram curves of PCF3, PCF4, and PCF5. The melting peak was due to the crystalline PCL phase. The melting temperature (T_m) and the melting enthalpy (ΔH_m in J/g) of the nanocomposites are summarized in Table I. We observed that T_m slightly increased with increasing content of the Fe powders. This result shows that the Fe powders had little influence on T_m, and they only absorbed some heat during the test process. As reported previously,[33] the perfect PCL crystals had a ΔH_m of 140 J/g. The lower ΔH_m of all of the nanocomposites indicated that the PCL segment was partially crystallized, and the others were in the amorphous state.

The dispersion of the Fe powders was investigated by FESEM, and typical images of PFC5 are shown in Figure 4(a–d) in which all of the pictures are cross-sectional drawings. Figure 4(a,c) shows the secondary electron (SE) images, whereas Figure 4(b,d) shows the backscattered electron images (BSE). Because the specimen was cut by a knife, there was some stress tropism on the cross sections, which resulted in some oblique lines in Figure 4(a). In the BSE images, the visible bright points are Fe powders, and the gray parts are the polymer matrix. The Fe powders deposited at one side (bottom) of the SMP films during the formation procedure. Hence, the contents of Fe powders in the two sides of the nanocomposites were different. The side that contained the most Fe powder was named the Fe side, whereas the other side was named the polymer side. The thickness of the layer of Fe powders was about 250 μm (the thickness of PFC5 was 1.2 mm), and almost no Fe powders could be found in the other polymer part. The thickness of the layer of

Table I. DSC Data for the Three Specimens

Specimen	T_m (°C)	ΔH_m (J/g)
PCF3	57.4	57.8
PCF4	57.6	54.4
PCF5	58.2	48.9

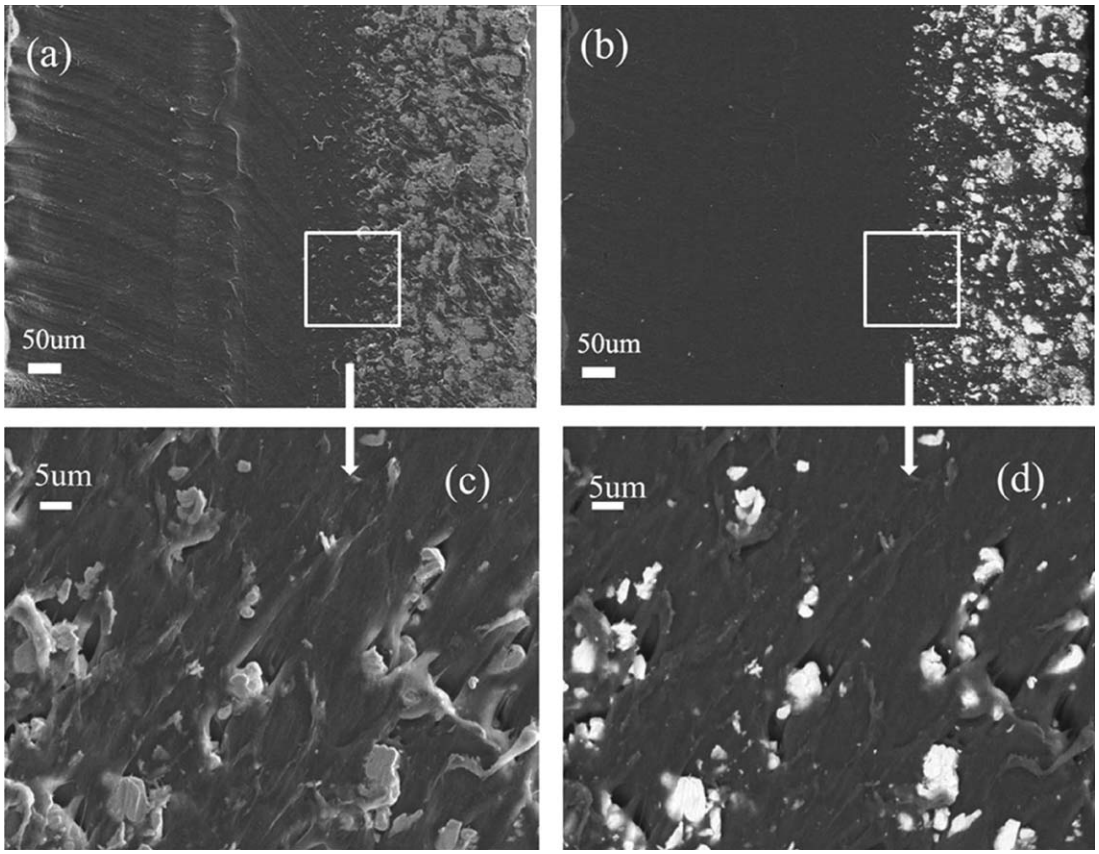

Figure 4. FESEM photographs: (a) PCF5 (SE), (b) PCF5 (BSE), (c) PCF5 (SE), and (d) PCF5 (BSE).

the Fe powders in PCF3 and PCF4 was about 200 μm, and the thicknesses of PCF3 and PCF4 were 0.9 and 1.1 mm, respectively. Figure 4(c,d) shows higher magnification images of the boundary between the layer of the Fe powders and the polymer part. Obviously, the Fe powders were wrapped in the polymer matrix. Hence, the adhered strength between the Fe powders and the polymer part was great.

Many researchers have found that the incorporation of a high content of filler particles in the polymer matrix had a negative effect on the mechanical properties.[17–19] If the particles are located on one side near the surface of the composites, however, the mechanical properties may not decrease. Because the Fe powders were gradually distributed in the nanocomposites, as shown in Figure 4, they had little influence on the polymer part. As a result, the nanocomposites had good mechanical properties. The tensile strength and elongation at break of the nanocomposites are summarized in Table II. According to the data, all of the samples showed high values of tensile strength and elongation at break; this indicated that they had good toughness. Compared with previously prepared nanocomposites, in which the Fe_3O_4 nanoparticles uniformly dispersed in the polymer matrix,[22] the mechanical properties of the functional gradient Fe/MWCNT-crosslinked polyurethane nanocomposites improved.

Table II. Mechanical Properties of the Nanocomposites

Specimen	Tensile strength (MPa)	Elongation at break (%)
PCF3	21.67 ± 0.87	2181.49 ± 193.36
PCF4	22.40 ± 0.12	2181.13 ± 109.75
PCF5	21.51 ± 0.80	2023.39 ± 120.52

The room-temperature magnetic hysteresis loops of the Fe powders and the nanocomposites are shown in Figure 5. A higher

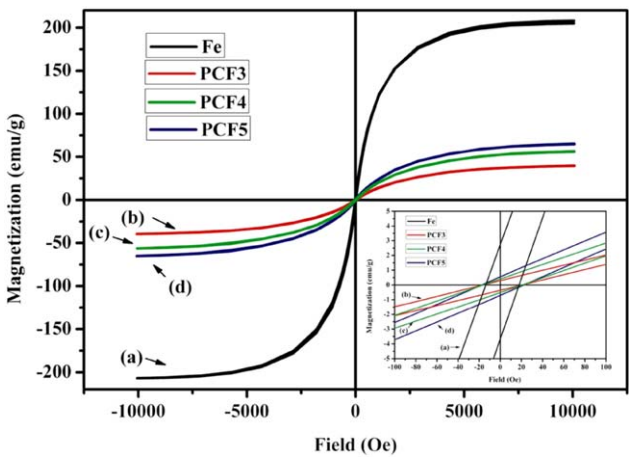

Figure 5. Magnetic hysteresis loops at room temperature: (a) Fe, (b) PCF3, (c) PCF4, and (d) PCF5. [Color figure can be viewed in the online issue, which is available at wileyonlinelibrary.com.]

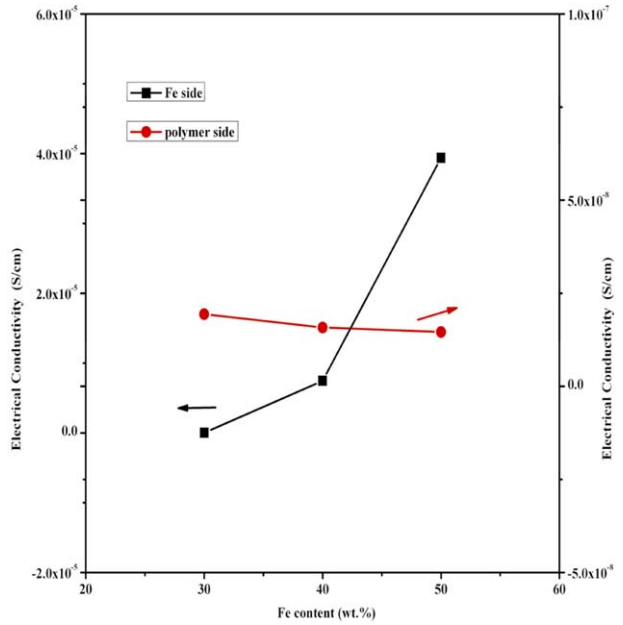

Figure 6. Electrical conductivities of samples with different Fe contents. [Color figure can be viewed in the online issue, which is available at wileyonlinelibrary.com.]

magnification image within a 100 Oe range is inserted in Figure 5 as well. The saturation magnetizations of the Fe powders, PCF3, PCF4, and PCF5 were 207.9, 39.6, 56.4, and 65.3emu/g, respectively. Because the polymer part had no magnetic properties, the nanocomposites had low saturation magnetizations, which were close to theoretical values. On the whole, the nanocomposites showed good magnetic properties. It could be expected that these nanocomposites would show a good magnetically induced SME in alternating magnetic fields.

Being metal, the Fe powders had a high electrical conductivity as well. Because we incorporated Fe powders into MWCNT-crosslinked polyurethane nanocomposites, the electrical conductivity of the nanocomposites may have improved a lot. A Hall effect measurement system was used to measure the electrical conductivity on each side of the nanocomposites. The electrical conductivities are shown in Figure 6. As shown in Figure 6, the Fe side has better electrical conductivities. The electrical conductivities on the Fe side of the PCF3, PCF4, and PCF5 were 2.26×10^{-8}, 7.46×10^{-6}, and 3.94×10^{-5} S/cm, respectively. With increasing content of Fe powders, the electrical conductivity improved significantly. Because of the increased Fe powders on the Fe side, there were more conductive paths formed between the Fe powders and MWCNTs in the nanocomposites. Hence, more electrons may easily passed through the sample, and the electrical conductivity was higher. However, on the polymer side, the electrical conductivity was low. The electrical conductivities on the polymer side of PCF3, PCF4, and PCF5 were 1.94×10^{-8}, 1.58×10^{-8}, and 1.46×10^{-8}S/cm, respectively. Because there was almost no Fe powder on this side, the electrical conductivities on the polymer side were much lower than those on the Fe side. Because of the magnetic properties and electrical conductivity of the nanocomposites, these functional gradient Fe/MWCNT-crosslinked polyurethane nanocomposites may have the opportunity to be used as electromagnetic shielding materials or sensors.

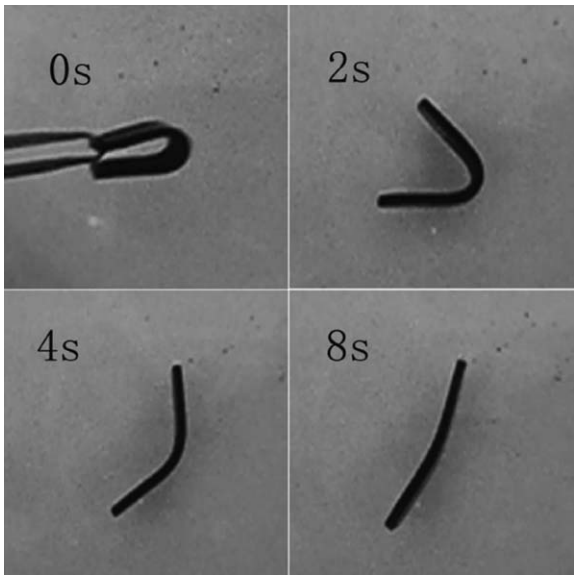

Figure 7. Shape-recovery process for PCF5 (Fe side inside) in hot water (45°C).

In all of our experiments of shape recovery of the nanocomposites, the folded samples were exposed at room temperature for 5 min. During this period of time, θ_f remained higher than 178°. Therefore, the R_f values of all of the samples were over 99%. A typical shape-recovery process of PCF5 (Fe side inside) in 45°C hot water is shown in Figure 7. The average values of the shape-recovery time and R_r of the three samples are listed in Table III. On the whole, there was little difference in the shape-memory properties of the nanocomposites induced by direct temperature heating. However, the shape-memory properties of the folded samples in which the Fe side was located on the inside were better than those of the folded samples in which the Fe side was located on the outside. Generally, metals have high thermal conductivity. When the Fe side was located inside the folded samples, the high-density Fe powders may have let the inside part of the folded samples obtain more heat energy, and the inside inner stress released first. Hence, there existed a promotion of shape recovery, and the shape-memory properties were better.

Table III. Shape-Memory Properties of the Nanocomposites (Fe Inside) in Hot Water (45°C)

Fe side location	Specimen	Recovery time (s)	R_r (%)
Inside	PCF3	8.67 ± 0.47	96.48 ± 0.52
	PCF4	8.67 ± 0.47	96.30 ± 0.26
	PCF5	8.00 ± 0.82	96.67 ± 0.52
Outside	PCF3	9.33 ± 0.94	94.63 ± 0.94
	PCF4	9.33 ± 0.47	95.19 ± 0.26
	PCF5	9.33 ± 0.47	95.74 ± 0.26

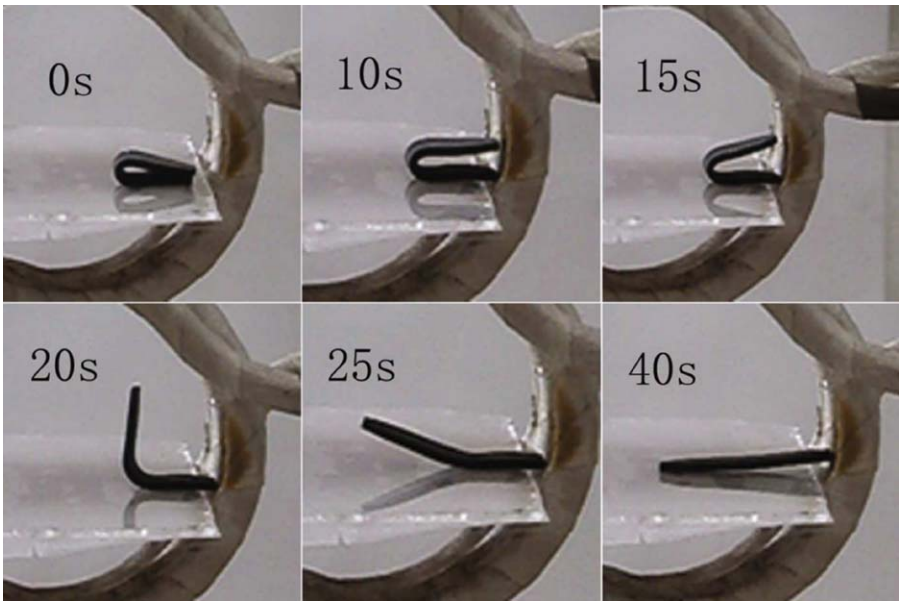

Figure 8. Typical shape-recovery process for PCF5 (Fe side inside) in a magnetic field ($f = 45$ kHz, $H = 46.5$ kA/m). [Color figure can be viewed in the online issue, which is available at wileyonlinelibrary.com.]

Figure 8 shows a typical shape-recovery process of PCF5 (Fe side inside) in an alternating magnetic field ($f = 45$ kHz, ($H = 46.5\text{kA}\cdot\text{m}^{-1}$). The whole process was about 40 s, and R_r was 97.41%. The data of the testing samples are listed in Table IV. When the samples were exposed to the alternating magnetic field, a period of time was needed to let the temperatures of the nanocomposites reach T_{trans}. This period of time was called the *magnetic field response time*. During this period of time, no obvious change was observed. When temperatures reached T_{trans}, the shape of the nanocomposites changed quickly. As shown in Table IV, the shape-recovery time of the nanocomposites decreased with increasing content of Fe powder, whereas R_r increased. As reported,[34] the magnetic particles could generate heat in an alternating field because of power loss. Enough generated heat allowed the temperatures of the SMPs to reach their T_{trans}. Therefore, PFC5 with the highest magnetic properties could absorb more heat energy in the same magnetic field than the other samples. Hence, it showed the shortest recovery time. The decreased R_r was due to the stress relaxation and creep. In comparison with the shape-memory properties in 45°C hot water, there was a similar result where the shape-memory properties were worse when the Fe side was located outside of the folded samples. The magnetic field response time and recovery time increased, and R_r decreased. When the Fe side was located outside of the folded samples, it took some time that for the generated heat to transfer from the outside to the inside. The shape recovery could be seen only when the inside temperature of the folded samples reached T_{trans}. Therefore, the magnetic response time increased. At the same time, the outside temperature of the folded samples already reached T_{trans}, and part of the inner stress was released. The released outside inner stress was not fully used, and the rest of the inner stress of the nanocomposites was not enough to realize the all of the shape recovery. Hence, R_r was lower. When the Fe side was located inside of the folded samples, the inside part of the nanocomposites could obtain more heat energy, and the inside inner stress released first; this promoted the shape recovery. With the inner stress was released from inside to outside, the inner stress was fully used, and R_r was relative higher. The temperature at which the shape-recovery process started for each sample was about 42°C, and the ending temperature was about 53°C.

Table IV. Shape-Memory Properties of the Nanocomposites in an Alternating Magnetic Field[a]

Fe side location	Specimen	Magnetic field response time (s)	Recovery time (s)	R_r (%)
Inside	PFC3	5.67 ± 0.47	82.00 ± 1.62	95.74 ± 0.26
	PFC4	2 ± 0	43.33 ± 3.40	96.85 ± 0.26
	PFC5	2 ± 0	40.00 ± 1.63	97.41 ± 0.26
Outside	PFC3	11.67 ± 0.47	109.00 ± 5.35	93.52 ± 0.26
	PFC4	6 ± 0.82	50.00 ± 0.82	95.19 ± 0.26
	PFC5	6 ± 0.82	42.67 ± 1.25	95.74 ± 0.26

[a] $f = 45$ kHz, $H = 46.5\text{kA}\cdot\text{m}^{-1}$.

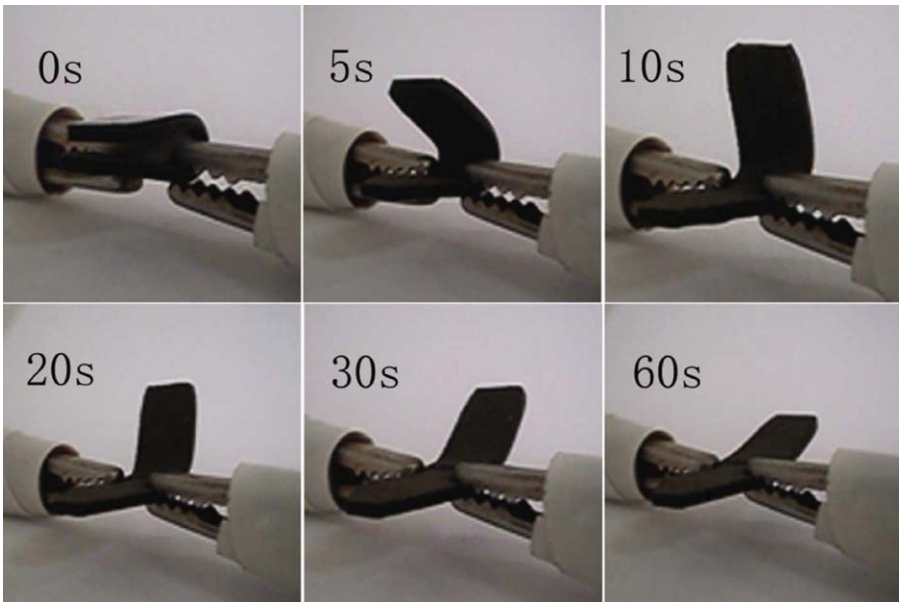

Figure 9. Electric-field-triggered shape recovery (30 V) of PCF5 (Fe side inside). [Color figure can be viewed in the online issue, which is available at wileyonlinelibrary.com.]

The electric-field-triggered shape recovery of PCF5 (with the Fe side being inside) is shown in Figure 9. Under a dc voltage of 30 V, the shape recovery could be clearly seen. The shape-recovery time was about 60 s, and R_r was $87.96 \pm 2.5\%$. The starting temperature of the shape-recovery process was about 42°C, and the ending temperature was about 50°C. However, at the same voltage, no shape recovery could be actuated for PFC3 and PFC4. This means that at such a voltage, the inside particles in the PFC3 and PFC4 nanocomposites could not generate enough heat to let the temperatures reach T_{trans}. The main reason was the low electrical conductivities of those samples. Because the electrode contacted two sides of the folded samples during the shape-recovery process, there was no obvious difference in the shape-memory properties when the Fe side was located inside or outside of the folded sample. The shape-recovery time was about 60 s, and R_r was about $87.04 \pm 2.77\%$ when the Fe side was located outside of the folded samples.

CONCLUSIONS

In this study, we demonstrated a simple way to produce functional gradient Fe/MWCNT-crosslinked polyurethane nanocomposites by an *in situ* polymerization method. The Fe powders were distributed in a gradient in the nanocomposites, and the polymer part was affected little; this resulted in good mechanical properties in the nanocomposites. The electrical conductivities on each side of the functional gradient nanocomposites were different; this indicated that the nanocomposites could be used as electromagnetic shielding materials or sensors. The shape-memory properties were dependent on the location of the Fe side, and the nanocomposites showed better shape-memory properties when the Fe side located on the inside of the folded samples. The shape-memory test indicated that the SME of the nanocomposites could be induced by temperature heating, Joule heating, and magnetic field heating. Such a kind of SMP composite might be used as intelligent material.

ACKNOWLEDGMENTS

This work was supported by the National Natural Science Foundation of China (contract grant number 21173084), the Shanghai Nanotechnology Promotion Center (contract grant number 0852 nm03200), and the Large Instruments Open Foundation of East China Normal University.

REFERENCES

1. Meng, Q.; Hu, J. *Compos. A* **2009**, *40*, 1661.
2. Hearon, K.; Gall, K.; Ware, T.; Maitland, D. J.; Bearinger, J. P.; Wilson, T. S. *J. Appl. Polym. Sci.* **2011**, *121*, 144.
3. Xue, L.; Dai, S.; Li, Z. *Biomaterials* **2010**, *31*, 8132.
4. Zuber, M.; Zia, K. M.; Barikani, M. *Adv. Struct. Mater.* **2013**, *18*, 55.
5. Barikani, M.; Zia, K. M.; Bhatti, I. A.; Zuber, M.; Bhatti, H. N. *Carbohydr. Polym.* **2008**, *74*, 621.
6. Zia, K. M.; Zuber, M.; Mahboob, S.; Sultana, T.; Sultana, S. *Carbohydr. Polym.* **2010**, *80*, 229.
7. Zia, K. M.; Zuber, M.; Barikani, M.; Bhatti, I. A.; Khan, M. B. *Colloids Surf. B* **2009**, *72*, 248.
8. Lendlein, A.; Langer, R. *Science* **2002**, *296*, 1673.
9. Yang, D.; Huang, W.; Yu, J.; Jiang, J. S.; Zhang, L. Y.; Xie, M. R. *Polymer* **2010**, *51*, 5100.
10. Leng, J.; Zhang, D. W.; Liu, Y. J.; Yu, K.; Lan, X. *Appl. Phys. Lett.* **2010**, *96*, 111905.
11. Lee. H. F.; Yu, H. H. *Soft Matter* **2011**, *7*, 3801.
12. Luo, X. F.; Mather, P. T. *Soft Matter* **2010**, *6*, 2146.

13. Jung, Y. C.; Yoo, H. J.; Kim, Y. A.; Cho, J. W.; Endo, M. *Carbon* **2010**, *48*, 1598.
14. Mohr, R.; Kratz, K.; Weigel, T.; Lucka-Gabor, M.; Moneke, M.; Lendlein, A. *Proc. Natl. Acad. Sci.* **2006**, *103*, 3540.
15. Razzaq, M. Y.; Behl, M.; Kratz, K.; Lendlein, A. *Mater. Res. Soc. Symp. Proc.* **2009**, 1140, HH05.
16. Golbang, A.; Kokabi, M. *Adv. Mater. Res.* **2010**, *123*, 999.
17. Yang, D.; Huang, W.; He, X. H.; Xie, M. R. *Polym. Int.* **2012**, *61*, 38.
18. Zheng, X. T.; Zhou, S. B.; Xiao, Y.; Yu, X. J.; Li, X. H.; Wu, P. Z. *Colloid Surf. B* **2009**, *71*, 67.
19. Yakacki, C. M.; Satarkar, N. S.; Gall, K.; Likos, R.; Hilt, J. Z. *J. Appl. Polym. Sci.* **2009**, *112*, 3166.
20. Buckley, P. R.; McKinley, G. H.; Wilson, T. S.; Small, W.; Benett, W. J.; Bearinger, J. P.; McElfresh, M. W.; Maitland, D. *J. IEEE Trans. Biol. Med. Eng.* **2006**, *53*, 2075.
21. Kumar, U. N.; Kratz, K.; Wagermaier, W.; Behl, M.; Lendlein, A. *J. Mater. Chem.* **2010**, *20*, 3404.
22. Cai, Y.; Jiang, J. S.; Zheng, B.; Xie, M. R. *J. Appl. Polym. Sci.* **2013**, *127*, 49.
23. Lu, H. B.; Liu, Y. J.; Gou, J. H.; Leng, J. S.; Du, S. Y. *Smart Mater. Struct.* **2010**, *19*, 075021.
24. Yu, K.; Zhang, Z. C.; Liu, Y. J.; Leng, J. S. *Appl. Phys. Lett.* **2011**, *98*, 074102.
25. Leng, J. S.; Lan, X.; Liu, Y. J.; Du, S. Y. *Smart Mater. Struct.* **2009**, *18*, 074003.
26. Xiao, Y.; Zhou, S. B.; Wang, L.; Gong, T. *ACS Appl. Mater. Interfaces* **2010**, *2*, 3506.
27. Jimenez, G. A.; Jana, S. C. *Polym. Eng. Sci.* **2009**, *49*, 2020.
28. Lu, H. B.; Gou, J. H.; Leng, J. S.; Du, S. Y. *Smart Mater. Struct.* **2011**, *20*, 035017.
29. Leng, J. S.; Lan, X.; Liu, Y. J.; Du, S. Y.; Huang, W. M.; Liu, N.; Phee, S. J.; Yuan, Q. *Appl. Phys. Lett.* **2008**, *92*, 014104.
30. Geng, C. H.; Cheng, R. M.; Xu, X. C.; Chen, Y. W. *J. Funct. Mater.* **2004**, *35*, 2853.
31. Liu, Y. Y.; Han, C. M.; Tan, H. F.; Du, X. W. *Mater. Sci. Eng. A* **2010**, *527*, 2510.
32. Zia, K. M.; Bhatti, I. A.; Barikani, M.; Zuber, M.; Bhatti, H. N. *Carbohydr. Polym.* **2009**, *76*, 183.
33. Ping, P.; Wang, W. S.; Chen, X. S.; Jing, X. B. *J. Polym. Sci. Part B: Polym. Phys.* **2007**, *45*, 557.
34. Razzaq, M.; Anhalt, M.; Frormann, L.; Weidenfeller, B. *Mater. Sci. Eng. A* **2007**, *444*, 227.